

1 **Investigating the ‘Atypical Rhythm Risk’ hypothesis in children with**  
2 **developmental language disorder using an EEG rhythmic speech paradigm**

3

4 Mahmoud Keshavarzi<sup>1</sup>, Susan Richards, Georgia Feltham, Lyla Parvez and Usha Goswami

5

6

7

8 Centre for Neuroscience in Education, Department of Psychology, University of Cambridge,  
9 Cambridge, CB2 3EB, United Kingdom

10

11

12

13

14

15

16

17

18

19

20

21 <sup>1</sup>Corresponding Author: [mk919@cam.ac.uk](mailto:mk919@cam.ac.uk), [Mahmoud.keshavarzi.ir@ieee.org](mailto:Mahmoud.keshavarzi.ir@ieee.org)

## 22 **Abstract**

23 Sensitivity to rhythmic and prosodic cues in speech has been described as a precursor of  
24 language acquisition. Consequently, atypical rhythmic processing during infancy and early  
25 childhood has been considered a risk factor for developmental language disorders. This is the  
26 ‘atypical rhythm risk’ (ARR) hypothesis. The neural processing of rhythmic speech has not yet  
27 been explored in children with developmental language disorder (DLD). Here we utilise EEG  
28 and a rhythmic speech paradigm previously utilised for dyslexia to investigate the ARR  
29 hypothesis in 9-year-old children with and without DLD. We investigate angular velocity,  
30 power, ERPs, phase-amplitude coupling (PAC) and phase-phase coupling (PPC), at three  
31 frequency bands, delta, theta and low gamma. Both groups demonstrated significant and  
32 equivalent phase entrainment in the delta and theta bands, but only the control children showed  
33 significant phase entrainment in the low gamma band. Further, while angular velocity in the  
34 delta and theta bands was equivalent by group, there was a significant gamma-band difference.  
35 The children with DLD also exhibited significantly more theta and gamma power compared to  
36 the control children. Regarding PAC and PPC, both groups showed significant and equivalent  
37 coupling strength. However, group resultant phase differences showed that low-frequency  
38 phase (delta and theta) affected gamma oscillations differently by group. The EEG data show  
39 important differences between children with and without DLD in the neural mechanisms  
40 underpinning the processing of rhythmic speech. The findings are discussed in terms of  
41 auditory theories of DLD.

42

## 43 **Keywords**

44 Developmental language disorder, rhythmic audio-visual speech, EEG, neural phase  
45 entrainment, atypical rhythm risk

## 46 **1. Introduction**

47 A growing number of cognitive behavioural studies have investigated rhythmic and/or musical  
48 processing in children with developmental language disorder (DLD), and have shown that  
49 atypical rhythm processing is associated with speech and language processing problems (e.g.,  
50 Corriveau et al., 2007; Corriveau & Goswami, 2009; Przybylski et al., 2013; Cumming et al.,  
51 2015a,b; Richards & Goswami, 2015, 2019; Sallat & Jentschke, 2015; Bedoin et al., 2016).  
52 This apparent link between rhythm processing and language processing has been described by  
53 the Atypical Rhythm Risk (ARR) hypothesis (Ladányi et al., 2020). Following a review of the  
54 literature, Ladányi et al. (2020) proposed that individuals with atypical rhythm processing are  
55 at higher risk for developmental speech/language disorders, including developmental dyslexia,  
56 DLD and stuttering. Disordered development of oral language (DLD) affects between 3 – 7%  
57 of children in all cultures (Bishop et al., 2017). The clinical diagnosis for such children was  
58 previously Specific Language Impairment (SLI), however the multinational and  
59 multidisciplinary CATALISE study recommended a change in terminology to DLD (Bishop et  
60 al., 2017). Children given a diagnosis of DLD have a range of language difficulties that cause  
61 functional impairments in their daily lives, yet have no known biomedical aetiology. The core  
62 dimensions of difficulty are problems with syntax and grammar, problems with word  
63 semantics, impairments in verbal memory and problems with phonology (see Leonard, 2014;  
64 Bishop, 2013). The possibility that atypical *neural* processing of rhythm is associated with  
65 DLD has not yet been investigated, and is the focus of the current study.

66 At the sensory/neural level, the ARR hypothesis is captured by Temporal Sampling (TS)  
67 theory (Goswami, 2011; 2015, 2022). TS theory was originally proposed to explain the  
68 rhythmic impairments found in children with developmental dyslexia, a disorder of written  
69 language processing that presents with core phonological impairments (Stanovich, 1988; Swan  
70 & Goswami, 1997; Snowling, 2000). Prior TS-driven behavioural studies of rhythmic

71 processing by children with dyslexia and children with DLD have shown many similarities,  
72 such as impaired sensory discrimination of amplitude rise times (important acoustic cues to  
73 rhythm, Corriveau et al., 2007; Corriveau & Goswami, 2009; Fraser et al., 2010; Beattie &  
74 Manis, 2012; Cumming et al., 2015a; Richards & Goswami, 2015, 2019) and relative  
75 insensitivity to syllable stress patterns in words and phrases (Cumming et al., 2015a,b; Richards  
76 & Goswami, 2015, 2019). TS theory suggests that the sensory/neural processing of rhythm is  
77 impaired because acoustic processing of the amplitude envelope of both speech and musical  
78 signals is atypical in children with developmental disorders of language, particularly at  
79 amplitude modulation rates <10 Hz that are known to carry information about rhythm and (for  
80 speech) syllable stress patterns (see Greenberg, 2006). The amplitude envelope of speech is  
81 known to be tracked cortically, possibly via entrainment of endogenous low-frequency  
82 oscillations <10 Hz (corresponding to the electrophysiological delta and theta bands, 0.5-4 Hz  
83 and 4-8 Hz, respectively) to the speech envelope (Giraud & Poeppel, 2012). Regarding the  
84 neural side of TS theory, prior TS studies with dyslexic children have documented neural  
85 differences compared to typically-developing (TD) children during the processing of both  
86 speech and non-speech rhythmic stimuli (Power et al., 2013; Keshavarzi et al., 2022; Peter et  
87 al., 2022). For speech stimuli, children's neural processing of rhythm has been investigated  
88 using the syllable repetition task (Power et al., 2012). In this task, EEG is recorded while  
89 children with dyslexia listen to the speech syllable "ba" presented audio-visually at a repetition  
90 rate of 2 Hz (Power et al., 2013; Keshavarzi et al., 2022). Both 9-year-old (Keshavarzi et al.,  
91 2022) and 13-year-old (Power et al., 2013) children with dyslexia show atypical delta-band  
92 phase synchronisation in the syllable repetition task, exhibiting a different preferred phase to  
93 children without dyslexia for the delta band only. The theta and alpha bands are not affected.  
94 Both Power et al. (2013) and Keshavarzi et al. (2022) reported that neural responding in the  
95 delta band was aligned to a different temporal point for each group, despite the highly

96 predictable rhythmic input. These studies suggest that there is an optimal (or preferred) phase  
97 of entrainment regarding the accurate and efficient processing of rhythmic inputs, and that this  
98 preferred phase differs in the dyslexic brain. To date, the rhythmic syllable repetition task has  
99 not been administered to children with DLD. We provide such a study here.

100         Prior neural studies of children with DLD have not to date employed rhythmic  
101 processing tasks nor investigated the TS framework. The absence of neural rhythm studies is  
102 surprising, as adult neural studies show that temporal prediction of the location of stressed  
103 syllables facilitates syntactic processing (Kotz & Schmidt-Kassow, 2015). Linguistic analyses  
104 show that adults produce a stressed syllable on average every 500ms, a “beat rate” of 2Hz  
105 (Dauer, 1983), a finding that underpins the choice of repetition rate in the current task. Prior  
106 DLD studies have instead primarily utilised fMRI and have sought structural and functional  
107 differences that may throw light on the aetiology of this developmental disorder. For example,  
108 there has been interest in whether hemispheric asymmetries during linguistic processing are  
109 different when children with DLD are compared to TD children (Bishop, 2013). While  
110 laterality per se has not proved conclusive (Parker et al., 2022), one of the most consistent  
111 findings in the functional fMRI literature with DLD children is that left frontal and temporal  
112 cortical areas show reduced activation during language processing (Asaridou & Watkins, 2022,  
113 for review). Children with DLD also show microstructural differences in dorsal anatomical  
114 pathways that connect frontal and temporal areas, as well as structurally-atypical basal ganglia  
115 (Badcock et al., 2012; Lee et al., 2013; Watkins et al., 2002). Although both the temporal areas  
116 and the basal ganglia are important for speech processing, speech motor learning and temporal  
117 prediction (see Kotz & Schmidt-Kassow, 2015), fMRI studies have not revealed which neural  
118 mechanisms associated with these areas could be affected in DLD. There are also prior EEG  
119 and MEG studies with DLD children, but again these studies have not adopted a rhythmic nor  
120 a speech tracking focus, and have not thrown light on underlying mechanisms (e.g. Shafer et

121 al., 2001). Many of the prior child EEG studies concern the overlap between DLD diagnoses  
122 and epileptic seizures (e.g. Mehta et al., 2015; Systad et al., 2019). However, a series of EEG  
123 studies with German-learning infants has shown that those at family risk for DLD show  
124 impaired neural ERP markers of language learning, such as a delayed N400 (thought to index  
125 semantic integration, Friedrich & Friederici, 2005, 2006). ERP studies with English-learning  
126 infants at family risk for DLD using a non-speech tone pair task have shown that at-risk infants  
127 have ERPs with larger amplitudes than TD infants when the tones follow each other rapidly in  
128 time (gap of 70 ms, Benasich et al., 2006), and also show a longer latency (in the N250) which  
129 is right-lateralized. Meanwhile, prior MEG studies of DLD using speech processing tasks are  
130 consistent with the functional fMRI literature in showing atypical left hemisphere temporal  
131 function (Helenius et al., 2009, 2014).

132 The TS framework (TSF) differs from these prior fMRI and MEG literatures in  
133 predicting impairments in right-lateralised neural mechanisms during language processing for  
134 children with DLD (Goswami, 2022, for review). However, the TSF is not based on laterality  
135 differences, rather the right hemisphere predictions arise from the nature of the neural  
136 mechanisms of speech encoding that are proposed to be impaired. These mechanisms involve  
137 the oscillatory encoding of slower amplitude modulation (AM) information in the speech  
138 amplitude envelope, also called cortical speech tracking. Slower AM information in speech is  
139 thought to be preferentially processed in the right hemisphere, while faster AM information is  
140 thought to be processed in the left hemisphere (Boemio & Poeppel, 2005; see also Rios-Lopez  
141 et al., 2020, 2022, for child data). For linguistic inputs, these hemispheric preferences appear  
142 to change during the acquisition of literacy when orthographic representations are acquired  
143 (Cutini et al., 2016; Lallier et al., 2017). TS theory proposes atypical sensory/neural processing  
144 of the slower rates of AM nested in the speech amplitude envelope (AE) for children with DLD  
145 (Goswami, 2011, 2015, 2022). The AE is the slow-varying energy contour of speech that aids

146 the perception of rhythm (Greenberg, 2006). The AE contains a range of AM patterns, created  
147 by hierarchical nesting of AMs at different temporal rates that are functionally connected by  
148 phase-phase and phase-power relations (Ghitza & Greenberg, 2009; Giraud & Poeppel, 2012;  
149 Goswami & Leong, 2013; Gross et al., 2013). For example, computational speech modelling  
150 studies show that the phase relations between these different AM rates (delta-theta, theta-  
151 beta/low gamma) provide systematic statistical cues to both phonological units such as stressed  
152 vs unstressed syllables, syllables, and onset-rimes (acoustic-emergent phonology, Leong &  
153 Goswami, 2015) and also to aspects of grammar such as plural marking (Flanagan & Goswami,  
154 2018). By TS theory, therefore, impaired cortical tracking of one or more of the AM rates nested  
155 in the AE, or of the phase-amplitude or phase-phase relations between different AM bands,  
156 could cause atypical development of one or more aspects of language.

157         Recent infant data support the linguistic predictions made by TS theory. In the  
158 Cambridge UK BabyRhythm project, 120 infants were followed longitudinally from the age of  
159 2 months, and EEG was recorded while the infants listened to either sung speech (nursery  
160 rhymes), to the rhythmic syllable repetition task, or to a matched drumbeat (nonspeech)  
161 rhythmic repetition task (Attaheri et al., 2022a,b; Ni Choisdealbha et al., 2022, 2023;  
162 Keshavarzi et al., 2023). In the syllable repetition task, infants showed evidence for a group  
163 preferred phase as early as 2 months of age, and by 6 months individual phase consistency was  
164 present over both left- and right-temporal regions as well as over parietal-occipital regions (Ni  
165 Choisdealbha et al., 2023). Individual phase angles predicted language acquisition at 18 months  
166 as measured by an infant-led vocabulary task (in this task, the infant selects one of two pictures  
167 that matches a spoken word, Ni Choisdealbha et al., 2023). In the rhythmic drumbeat  
168 (nonspeech) task, neural phase angle at 9 months predicted nonword repetition at 24 months, a  
169 phonological measure (Ni Choisdealbha et al., 2023). Accordingly, delta-band phase angles to  
170 both speech and nonspeech rhythmic stimuli predict later language outcomes for a TD sample.

171 For the nursery rhyme analyses, significant cortical tracking of the low-frequency envelope  
172 information was present in both delta and theta bands by 4 months of age, with no significant  
173 tracking present for faster bands (alpha band, see Attaheri et al., 2022a). Phase-amplitude  
174 coupling (PAC) between both delta and theta phase and beta and gamma amplitudes was  
175 present from 4 months, and showed no change over development for this sample. When  
176 language outcomes were assessed, only delta band cortical tracking and theta-gamma PAC  
177 predicted later vocabulary and phonology measured at 24 months (Attaheri et al., preprint).  
178 Grammar measures were included in the UK BabyRhythm study, but did not show sufficient  
179 individual differences for neural prediction analyses (Rocha et al., 2024). Nevertheless, these  
180 prior TSF-driven infant data suggest that both delta-band phase angle and theta-gamma PAC  
181 in the current study may be associated with DLD status.

182         There is also one prior study of rhythmic speech processing using a modulation band  
183 manipulation with children with DLD, which would predict atypical gamma band speech  
184 tracking. Goswami et al. (2016) used a nursery rhyme recognition task based on speech that  
185 was either low-pass filtered (< 4 Hz, providing delta band information only) or band-pass  
186 filtered (~33Hz, providing faster low gamma band modulations only) so that the speech input  
187 was degraded and difficult to recognise. The children's task was to recognise the matching  
188 nursery rhyme by making a selection in a picture-based multiple choice format. Goswami et  
189 al. reported that 9-year-old children with DLD were worse than TD age-matched children when  
190 selecting bandpass-filtered targets, but not when selecting low-pass filtered targets. Children  
191 with both DLD and dyslexia (DLD children with phonological impairments) were worse than  
192 TD children at recognising the nursery rhymes in both filtered speech conditions. All groups  
193 of children found it easier to recognise the low-pass filtered rhymes (e.g. children with DLD  
194 recognised 89% of the low-pass filtered rhymes compared to 42% of the bandpass filtered  
195 rhymes, while the TD children recognised 94% and 59% respectively). When relations with



196 language development were investigated in the full sample of 9-year-olds ( $N = 95$ ), accuracy  
197 in the bandpass-filtered speech condition was the stronger predictor of language outcomes,  
198 accounting for 12% of unique variance in the Clinical Evaluation of Language Fundamentals  
199 (CELF-III, Wiig, Semel & Secord, 2017) receptive language measures and 10% of unique  
200 variance in CELF expressive language scores. By contrast, accuracy in the low-pass filtered  
201 speech condition accounted for 9% of unique variance in the phonological measure (rhyme  
202 awareness), but only 3% of unique variance in the CELF ( $p < 0.05$ ). To interpret their data,  
203 Goswami et al. (2016) suggested that although prior TSF studies of children with dyslexia and  
204 children with DLD indicate a shared sensory difficulty in processing temporal modulation  
205 patterns in speech, the neural temporal integration windows that are most impaired may differ  
206 for each disorder. Children with DLD may have more difficulties with faster temporal  
207 integration windows in speech-based tasks (gamma band difficulties).

208         Accordingly, we explored a number of *a priori* predictions in the current study. First, on  
209 the basis of the shared behavioural rhythmic features of dyslexia and DLD and our prior TSF  
210 dyslexia data, we expected atypical delta-band entrainment (reduced phase consistency) and a  
211 different group preferred phase for the participants with DLD compared to the age-matched  
212 TD control children. However, given the filtered speech findings discussed above (Goswami  
213 et al., 2016), and in contrast to the earlier rhythmic syllable repetition studies of children with  
214 dyslexia (Power et al., 2013; Keshavarzi et al., 2022), gamma band oscillations were measured  
215 in the current study as well. Given Goswami et al.'s (2016) finding of rhythmic speech  
216 processing difficulties at faster modulation rates, a second prediction was possible gamma band  
217 oscillatory group differences. Third, on the basis of our TSF infant data, we tentatively  
218 predicted atypical theta-gamma PAC for the children with DLD. The prior study of children  
219 with dyslexia that explored angular velocity (Keshavarzi et al., 2022) had also reported that the  
220 group angular velocity in the delta band for the children with dyslexia was almost twice the

221 rate of the TD control group, suggestive of different changes in phase across time for the  
222 dyslexic group. Accordingly, a final tentative prediction was that angular velocity in the delta  
223 band may differ between children with and without DLD. We note that the prior literature on  
224 sensory impairments in rapid auditory non-speech (tone) processing in infants at family risk  
225 for DLD would also predict gamma band impairments for the DLD children (Ortiz-Mantilla &  
226 Benasich, 2013).

227

## 228 **2. Methods and materials**

### 229 **2.1. Participants**

230 Sixteen typically developing children (mean age of  $109 \pm 13$  months) and sixteen children with  
231 DLD (mean age of  $108 \pm 11$  months) took part in the study. All participants were taking part in  
232 an ongoing study of auditory processing in DLD and had English as the main language spoken  
233 at home (see Parvez et al., 2024). All participants exhibited normal hearing when tested with  
234 an audiometer. In a short hearing test across the frequency range 0.25 – 8 kHz (0.25, 0.5, 1, 2,  
235 4, 8 kHz), all children were sensitive to sounds within the 20 dB HL range. DLD status was  
236 assessed by administering two expressive and two receptive subtests of the CELF (Wiig, Semel  
237 & Secord, 2017). The subtests were recalling sentences, formulating sentences, and (depending  
238 on age) two of the word structure, sentence comprehension, word classes and semantic  
239 relationships subtests. Children who scored below the mean (7 or less when the mean score is  
240 10) on at least 2 of these subtests were included as DLD. The control children also received  
241 either one or two of the CELF tasks, recalling sentences ( $N = 16$ ) and formulating sentences  
242 ( $N = 11$ ) and scored in the normal range. The Picture Completion subtest of the Wechsler  
243 Intelligence Scale for Children (WISC IV, Wechsler, 2016) was used to assess non-verbal  
244 intelligence (NVIQ) and did not differ between groups. Group performance for the tasks  
245 administered to both groups is shown in Table 1.

246 **Table 1.** Details of the participating children, showing Scaled Scores (ScS, population mean  
247 = 10) and Standard Scores (SS, population mean = 100).

	DLD	Age-Matched Control (TD)
N	16	16
Age (months) <sup>A</sup>	108.3 (11.3)	108.9 (13.3)
Recalling Sentences ScS <sup>B</sup>	5.3 (1.7)	10.9 (2.3)
Formulating Sentences ScS <sup>B</sup>	4.4 (1.9)	10.8 (1.7)
WISC Picture Completion ScS <sup>A</sup>	7.9 (3.0)	9.9 (2.8)

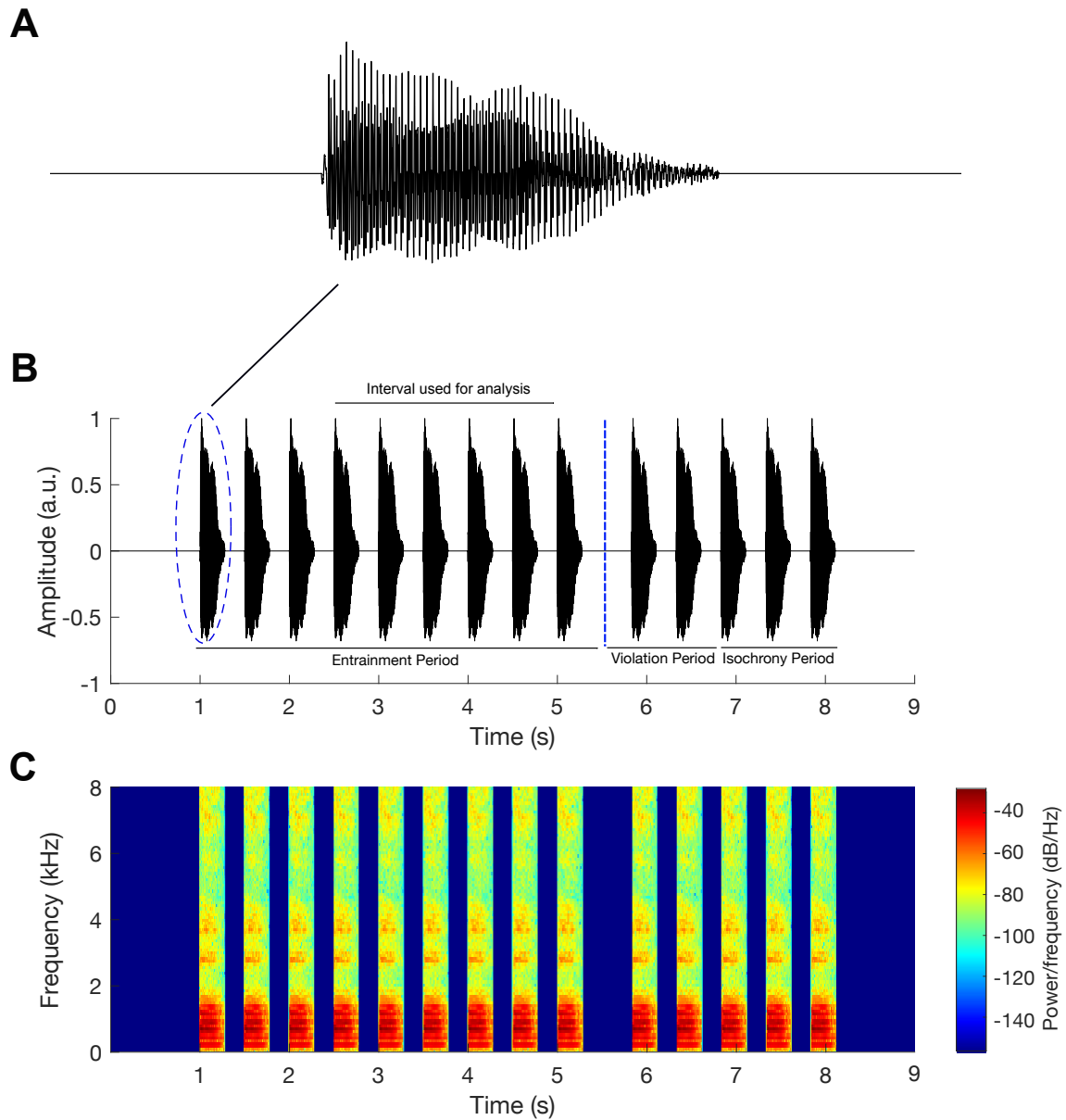
248 Note. **A:** TD and DLD groups are not significantly different; **B:** DLD group significantly worse than TD group,  $p$   
249  $< 0.01$ . WISC: Wechsler Intelligence Scale for Children.

250

## 251 **2.2. Experimental set up and stimuli**

252 The experimental set up and stimuli used in the EEG study were identical to those described  
253 by Keshavarzi et al. (2022, 2024). After putting the EEG cap, the children were seated in an  
254 electrically shielded soundproof room. They watched (on the screen) and listened (through  
255 earphones) to audio-visual stimuli and the EEG data were collected at a sampling rate of 1 kHz  
256 using a 128-channel EEG system (HydroCel Geodesic Sensor Net). The stimuli were a talking  
257 head presenting rhythmic sequences of the syllable “ba” at a rate of 2 Hz with both visual and  
258 additory information present. Visual cues began 68 ms before the onset of the stimulus “ba” as  
259 in natural speech. Each trial (sequence) consisted of sequence of 14 syllable “ba” with both  
260 visual and auditory information present (See Figure 1). One of the 14 syllables (either 9th, 10th  
261 or 11th syllable) in each trial could be out of time (rhythmic violation), in a random order. The  
262 temporal delay was calibrated individually and adaptively for each child, so that the oddball  
263 was detected around 79.4% of the time by a button press. Each child was presented with 90  
264 trials, 15 of which did not have a violation and were presented randomly as catch trials. Each  
265 trial contained three periods (see Figure 1): entrainment period, violation period, and return-  
266 to-isochrony period. Children were instructed to concentrate on the lips of the female face on  
267 the screen and to listen to the auditory stimuli. They were also asked to press a target key on  
268 the keyboard when one of the syllables was out of time. The total time for the EEG recording

269 (excluding the set-up) was about 15 min. Via the adaptive procedure, the success rate in the  
270 behavioural task was equated for all participants.  
271



272

273 Figure 1. Experimental stimuli. Panel A shows the waveform of a single syllable “ba”, panel B  
274 indicates an example trial (sequence of “ba” stimuli) with the violation at position of 10th  
275 stimulus, and panel C shows the spectrogram corresponding to sequence in panel B. This figure  
276 reproduced with permission from Keshavarzi et al., 2022.

277

### 278 2.3. EEG data pre-processing and analyses

279 The EEG data were first referenced to Cz and then band-passed filtered into 0.2 – 48 Hz using  
280 a zero phase FIR filter with low cutoff (–6 dB) of 0.1 Hz and high cutoff (–6 dB) of 48.1 Hz  
281 (EEGLab Toolbox; Delorme and Makeig, 2004). The bad channels were identified and  
282 interpolated using spherical interpolation (EEGLab Toolbox). The Independent Component  
283 Analysis (provided by EEGLab Toolbox) was run for each participant and the calculated  
284 independent components were then evaluated very carefully to remove artefactual components  
285 such as eye blinks and eye movements. The pre-processed EEG data were downsampled to  
286 100 Hz and band-pass filtered into delta (0.5 – 4 Hz), theta (4 – 8 Hz) and low gamma band  
287 (25 – 40 Hz) frequency bands (MNE Library-Python, Gramfort et al., 2013). The data were  
288 then epoched into individual trials, in the time interval of 0.5 s before the onset of the first “ba”  
289 stimulus and 4 s after that. In this study, the analyses only were focused on the EEG data  
290 corresponding to stimuli 4th-8th in the entrainment period of each trial to ensure that  
291 rhythmicity has occurred.

#### 292 **2.4. Computation of angular velocity**

293 The angular velocity,  $w(t)$ , for signal  $s(t)$  over time interval  $\Delta t = t_1 - t_2$  is calculated as:

$$294 \quad w(t) = \frac{\Delta\varphi_t}{\Delta t} \quad (1)$$

295 where  $\Delta\varphi_t$  refers to the changes in the instantaneous phase ( $\varphi(t)$ ) of the signal over the time  
296 interval  $\Delta t$ . The instantaneous phase is calculated as:

$$297 \quad \varphi(t) = \arctan\left(\frac{s_H(t)}{s(t)}\right) \quad (2)$$

298 where  $s_H(t)$  is the Hilbert transform of signal  $s(t)$ , and is calculated as:

$$299 \quad s_H(t) = \frac{1}{\pi} \int_{-\infty}^{\infty} \frac{s(\tau)}{t-\tau} d\tau \quad (3)$$

#### 300 **2.5. Computation of phase entrainment**

301 To check the phase entrainment for each group in each frequency band, we performed the  
302 following steps (Keshavarzi et al., 2022):

303 (1) Calculating instantaneous phases of all 128 EEG channels at the times corresponding to  
304 onsets of the 5 “ba” stimuli (4th-8th) in each trial.

305 (2) Computing mean phase for each trial by averaging across the phase values obtained for all  
306 EEG channels and for the 5 “ba” stimuli in step 1. This resulted in a single-phase value for  
307 each trial.

308 (3) Considering a single unit vector whose angle is determined by the phase value obtained in  
309 step 2 for each trial.

310 (4) Calculating the mean vector for each child by averaging across the unit vectors in step 3.  
311 This resulted in a single vector for each child, called *child resultant vector*.

312 (5) Considering a single unit vector whose angle is determined by the phase of *child preferred*  
313 *vector* in the vector space for each child.

314 (6) Calculating the mean vector for each group by averaging across the unit vectors obtained  
315 in step 5. This results in a single vector, called *group resultant vector*, for each group.

## 316 **2.6. Computation of event related potential**

317 To obtain the time-domain ERP for each group and each frequency band, the following steps  
318 were conducted: (1) Calculating the mean voltage amplitude for each trial by averaging across  
319 the voltage amplitudes of all 128 pre-processed for that each trial; (2) Calculating the mean  
320 voltage amplitude for each participant by averaging across the mean voltage obtained (in step  
321 1) for all trials of that participant; (3) Calculating the ERP for each group by averaging across  
322 the mean voltage obtained (in step 2) for all participants in that group.

## 323 **2.7. Computation of the band-power**

324 To investigate the power of neural response over the entrainment period used for analysis, we  
325 calculated the power of EEG responses for each child and each group using in four steps: (1)  
326 Calculating the power of each EEG channel separately for each trial; (2) Calculating the power  
327 for each trial by averaging across power obtained (in step 1) for channels; (3) Calculating the

328 power for each participant by averaging across power obtained (in step 2) for all trials of that  
329 participant; (4) Calculating the power for each group by averaging across power values  
330 obtained (in step 2) for all children in that group.

### 331 **2.8. Computation of cross frequency phase-amplitude coupling**

332 Cross frequency phase-amplitude coupling refers to the modulation of amplitude of signal at a  
333 high frequency band by the phase of low frequency oscillation. Here we quantified the strength  
334 of this type of modulation using modulation index ( $MI$ ; Tort et al. 2008; Hülsemann, 2019):

$$335 \quad MI = \frac{KL(U, X)}{\log B} \quad (4)$$

336 where  $B$  (=18) is the number of bins,  $U$  refers to the uniform distribution,  $X$  is the distribution  
337 of the data, and  $KL(U, X)$  is Kullback–Leibler distance which is calculated as:

$$338 \quad KL(U, X) = \log B - H(P) \quad (5)$$

339 where  $H(\cdot)$  is the Shannon entropy and  $P$  is the vector of normalized averaged amplitudes per  
340 phase bin which is calculated as:

$$341 \quad P(j) = \frac{\bar{a}}{\sum_{k=1}^N \bar{a}_k}, \quad j = 1, \dots, N \quad (6)$$

342 where  $\bar{a}$  is the average amplitude of each bin,  $k$  refers to running index for the bins. Note that  
343  $P$  is a vector with  $N$  elements.

### 344 **2.9. Computation of cross frequency phase-phase coupling**

345 Cross-frequency phase-phase coupling (PPC) refers to the phase synchrony between  
346 oscillations in two frequency bands. PPC between two oscillations is a value between 0 and 1,  
347 calculated as:

$$348 \quad PPC = \frac{1}{T} \left| \sum_{t=1}^T e^{-j\Delta\varphi(t)} \right| \quad (7)$$

349 where  $|\cdot|$  refers to the absolute value operator,  $T$  is the number of time samples, and  $\Delta\varphi(t)$  is  
350 the phase difference, and is calculated as:

$$351 \quad \Delta\varphi(t) = \varphi_1(t) - \varphi_2(t) \quad (8)$$

352 where  $\varphi_1(t)$  is the instantaneous phase of first signal and  $\varphi_2(t)$  is the instantaneous phase of  
353 the second signal.

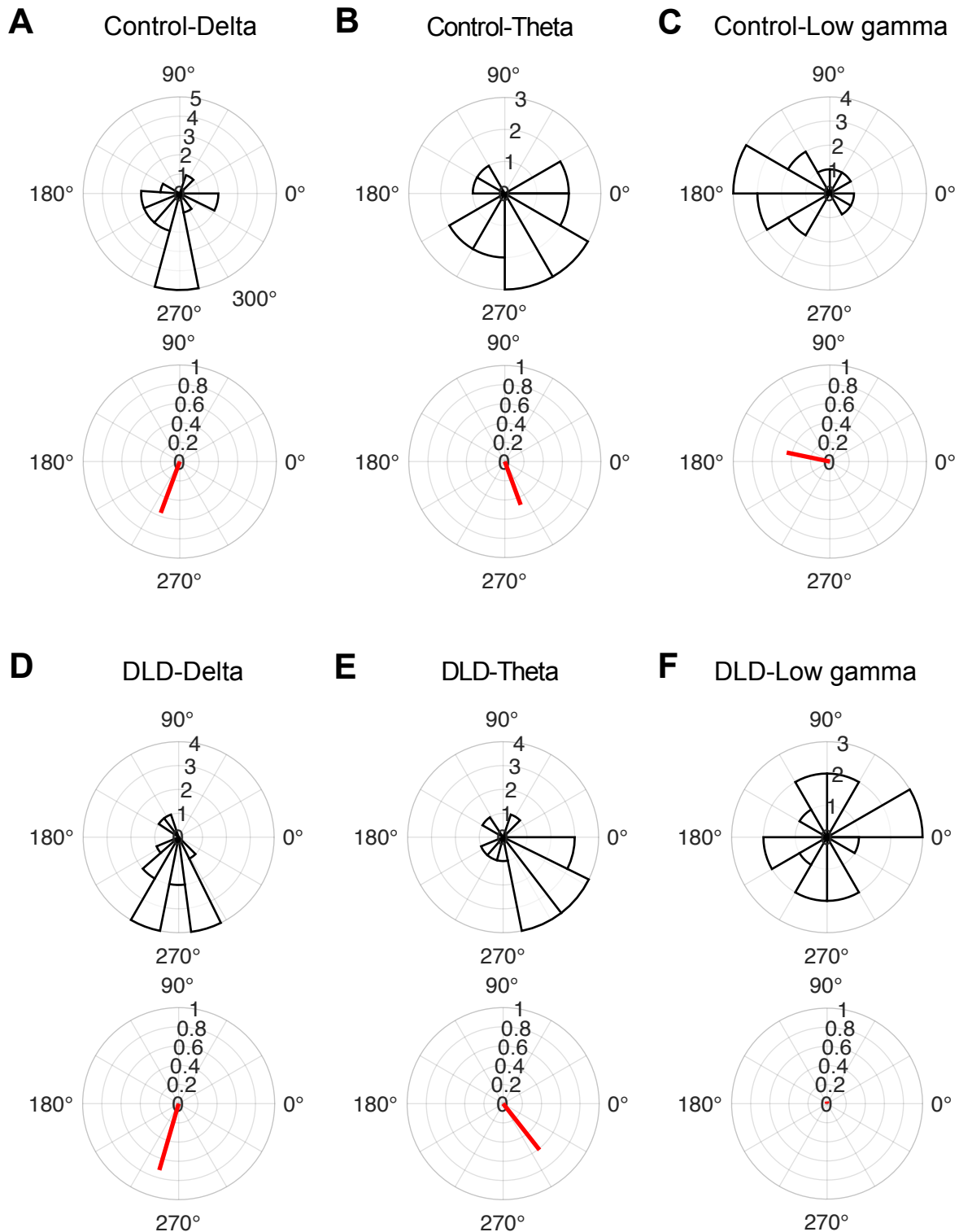
354

### 355 **3. Results**

#### 356 **3.1. Phase entrainment consistency in each group**

357 Given our prior TSF dyslexia data, we expected consistent phase entrainment in each group in  
358 the delta and theta bands. To assess the phase entrainment consistency in each group and in  
359 each frequency band, we applied the Rayleigh test of uniformity to the child preferred phases  
360 separately for each group and for each frequency band (see Figure 2). For the control children,  
361 we found consistency in all bands: delta band ( $z = 5.14$ ,  $p = 0.004$ , see Figure 2A), theta band  
362 ( $z = 3.70$ ,  $p = 0.022$ , see Figure 2B), and low gamma band ( $z = 3.33$ ,  $p = 0.033$ , see Figure 2C).  
363 For the children with DLD, we also found significantly consistent phase entrainment in the  
364 delta band ( $z = 8.31$ ,  $p = 8.35 \times 10^{-5}$ , see Figure 2D) and in the theta band ( $z = 6.00$ ,  $p = 0.0016$ ,  
365 see Figure 2E). However, phase consistency in the low gamma band was absent ( $z = 0.01$ ,  $p =$   
366  $0.99$ , see Figure 2F). This result indicates that the DLD brain does not show significant  
367 entrainment to rhythmic input in the gamma band.





368

369

370

371

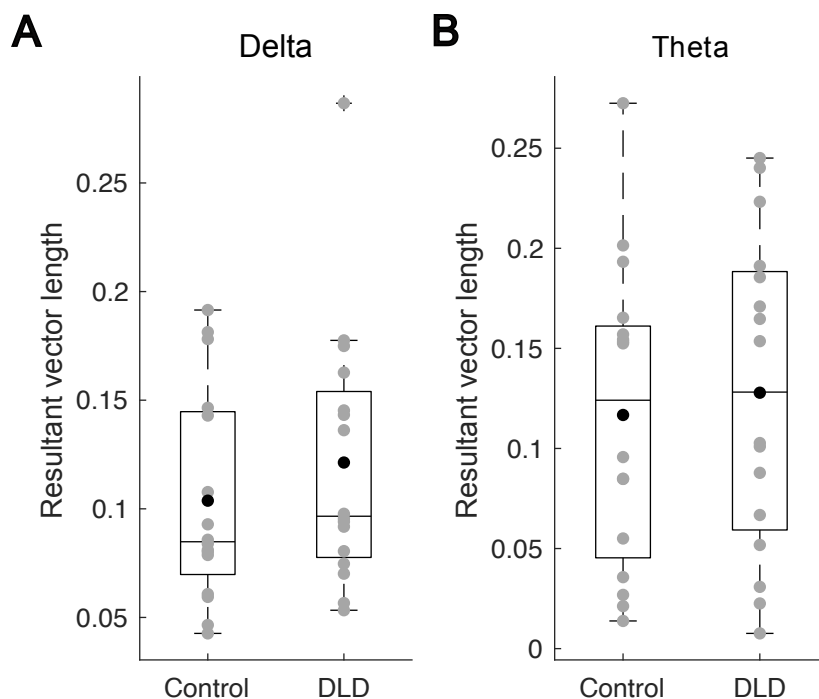
372

**Figure 2. Entrainment phase distribution across children in each group (rose plots) and group resultant vectors (red lines). Note the absence of phase consistency in the low gamma band for the children with DLD.**

373

### 3.2. Comparing the strength of phase entrainment between groups

374 *A priori*, we had expected the strength of the consistency of phase entrainment to differ by  
375 group in the delta band. The length of a *child resultant vector* can be considered as a criterion  
376 of the strength of phase entrainment across different trials for that child. Indeed, longer *child*  
377 *resultant vectors* indicate higher consistency of phase entrainment. To compare the strength of  
378 phase consistency in control children with children with DLD, we applied Wilcoxon rank sum  
379 tests based on the length of the *child resultant vectors* for the two frequency bands showing  
380 significant entrainment, delta and theta. Contrary to prediction, there was no significant  
381 difference between the two groups for either band (delta:  $z = -0.70$ ,  $p = 0.49$ , Figure 3A; theta:  $z$   
382  $= -0.55$ ,  $p = 0.58$ , Figure 3B). We also checked these comparisons after removing outliers. A  
383 data point was considered as an outlier if the corresponding power value was greater than a 1.5  
384 interquartile range above the upper quartile or below the lower quartile of the population data  
385 in that group. There were also no significant group differences after outlier removal.



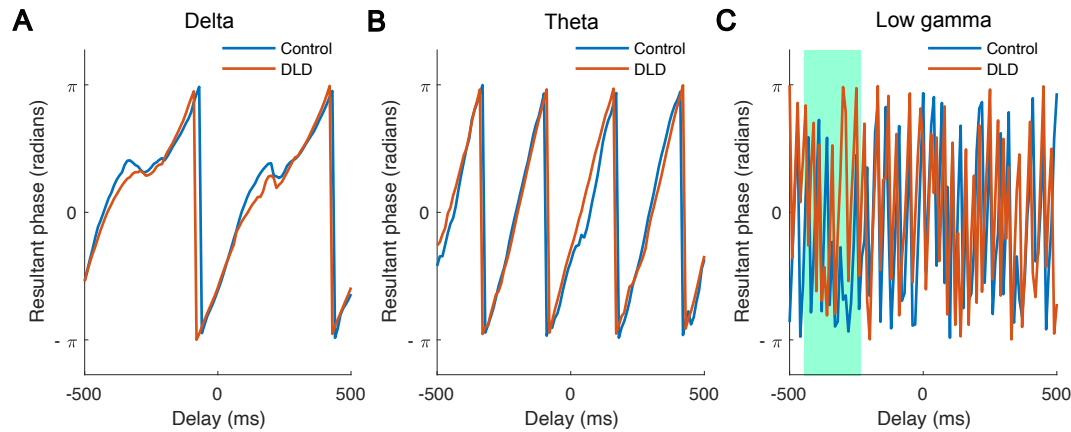
386  
387 **Figure 3. The length of child resultant vectors in the delta (A) and theta (B) bands in the**  
388 **two groups.** The grey circles denote the length of the child resultant vectors for individual  
389 participants, the black disks denote the mean values for each group, and the horizontal line on  
390 each box shows the median.  
391

### 392 3.3. Comparing preferred phase and angular velocity between groups

393 *A priori* we expected group differences in both preferred phase in the delta band and in angular  
394 velocity in the delta band. To compare preferred phase between groups, the Watson-Williams  
395 test was applied to the delta and theta band data. The low gamma band was excluded, as it did  
396 not show consistent phase entrainment for the children with DLD. The Watson-Williams test  
397 assumes von Mises distributions, although this test is fairly robust against deviations from this  
398 assumption (Zar, 1999; Berens, 2009). In our data, the phase distribution for both delta and  
399 theta bands, as well as for both groups (TD and DLD), followed von Mises distributions  
400 (Watson's U2 test,  $p > 0.05$ ). Contrary to prediction, there was no significant difference in terms  
401 of preferred phase between the groups, neither in the delta band (Watson-Williams test,  $p =$   
402 0.84) nor in the theta band (Watson-Williams test,  $p = 0.46$ ).

403 We also explored the behaviour of preferred phase across time separately for each group  
404 and each frequency band by computing angular velocities. Here the gamma band data could be  
405 included, as angular velocity (see Section 2.4) analyses do not require phase consistency. To  
406 this end, we calculated the group preferred phase for each frequency band prior to and after the  
407 occurrence of a stimulus (stimuli 4th–8th) in the entrainment period over the time interval of –  
408 500 ms to 500 ms. This time interval corresponds to two repetitions of the syllable “ba”. Figure  
409 4 shows the group preferred phase for the two groups and for delta, theta, and low gamma  
410 bands. For both groups, delta-band and theta-band group preferred phases appear to follow a  
411 quasiperiodic pattern, with a frequency of around 2 Hz for the delta band (angular velocity of  
412 4 rad/s, see Figure 4A) and a frequency of around 4 Hz for the theta band (angular velocity of  
413 8 rad/s, see Figure 4B). For the low gamma band, however, the pre-stimulus group preferred  
414 phase for children with DLD appears to be different from that of the control children. We  
415 therefore employed a two-sample t-test to find the time bins with a statistical difference in  
416 terms of angular velocity. The result suggested a significant difference between the two groups

417 over the time interval of  $-440$  ms to  $-240$  ms (two-sample t-test,  $p = 0.017$ , see Figure 4C).  
418 This suggests that phase changes differently across time for the children with DLD, in the  
419 gamma band only.



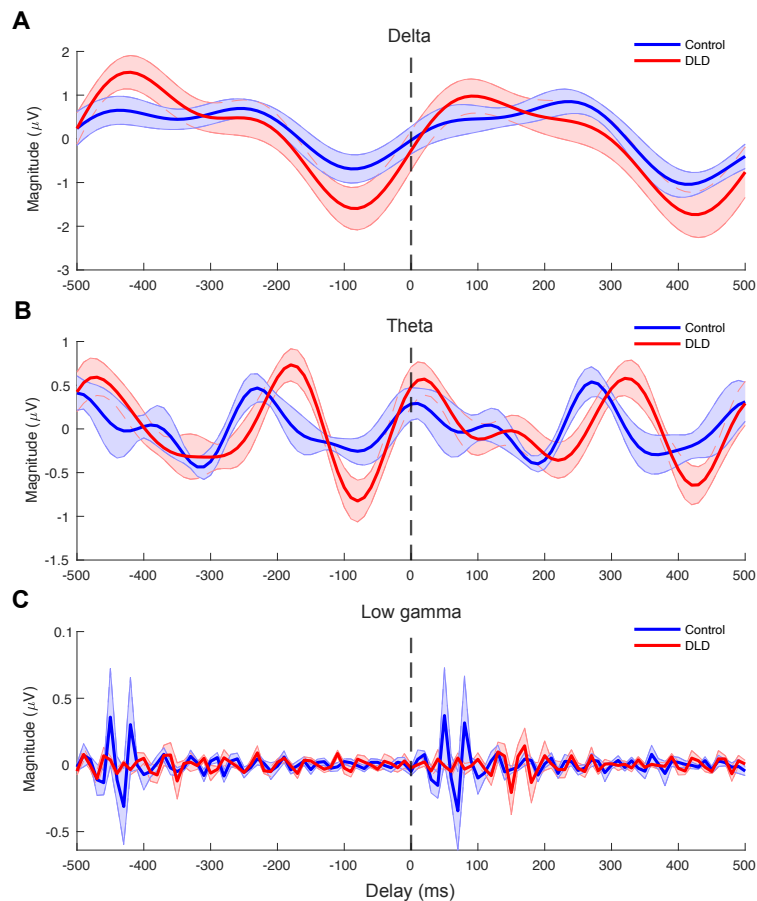
420  
421 **Figure 4. The group preferred phase (radians) as a function of the delay (ms) relative to**  
422 **the onset of “ba” stimuli.** The blue and red curves are related to control (N = 16) and DLD  
423 group (N = 16), respectively. Both curves appear to follow a quasiperiodic pattern with a  
424 frequency of around 2 Hz in the delta band (A) and a quasiperiodic pattern with a frequency  
425 rate of around 4 Hz in the theta band (B). The curves related to the low gamma band (C) reveal  
426 a pre-stimulus difference between the two groups. In particular, the pre-stimulus angular  
427 velocity in this band over the time interval of  $-440$  ms to  $-240$  ms (marked with green colour)  
428 differs significantly by group.

429

### 430 3.4. Comparing ERPs between groups

431 Figure 5 depicts the ERP curves for each group. We calculated the ERP in the time interval of  
432  $-500$  ms to  $500$  ms separately for each group and each frequency band, as described in Section  
433 2.6. Although differences between group could be expected in terms of pre- and post-stimulus  
434 peaks in ERPs from visual inspection of Figure 5, no significant group difference was found in  
435 any frequency band (delta, theta, low gamma).

436



437

438 **Figure 5. Event related potentials for delta (A), theta (B) and low gamma (C) bands.** The  
439 blue and red curves denote the ERPs for control and DLD groups, respectively. The shaded  
440 areas denote the standard error of mean for each group.

441

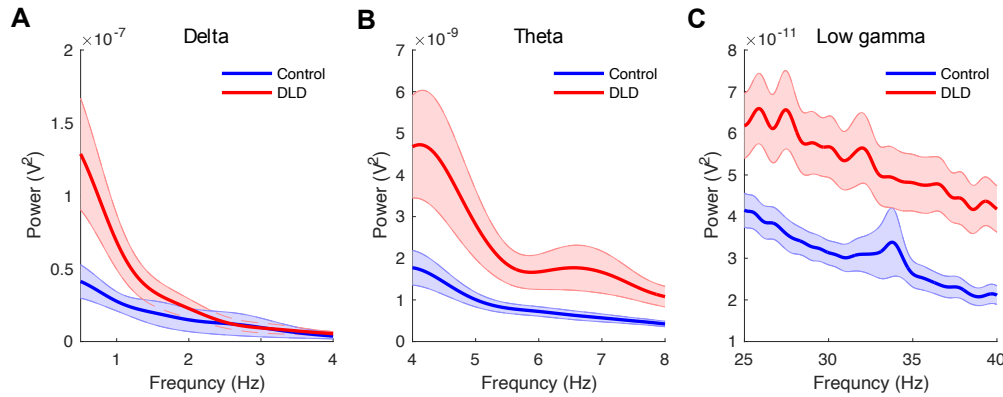
### 442 3.5. Comparison of band-power between groups

443 To compare the band-power between groups, Wilcoxon rank sum tests were applied for each  
444 frequency band after removing outliers. We calculated the average power over the entrainment  
445 period in each frequency band separately for each group, using steps described in Section 2.7.

446 Figure 6 shows the average power versus frequency separately for each group and for delta  
447 (see Figure 6A), theta (see Figure 6B), and low gamma (see Figure 6C) bands. A significant  
448 difference between control children and children with DLD was found in theta ( $z = -2.01$ ,  $p =$   
449  $0.04$ ; Figure 6B; outliers [control]  $N = 3$ , outliers [DLD]  $N = 2$ ;) and in low gamma ( $z = -2.64$ ,  
450  $p = 0.008$ ; Figure 6C; outliers [control]  $N = 2$ , outliers [DLD]  $N = 3$ ) bands. However, there

451 was no difference in band-power for the delta band ( $z = -1.45$ ,  $p = 0.15$ ; Figure 6A; outliers  
452 [control]  $N = 2$ , outliers [DLD]  $N = 2$ ).

453



454

455 **Figure 6. Delta-band (A), theta-band (B), and low gamma-band (C) power in the**  
456 **entrainment period.** The shaded areas denote the standard error of the mean for each group.  
457 Please note the numerical power differences in the y axis by band.

458

### 459 3.6. Comparing cross-frequency PAC between groups

460 *A priori*, we had tentatively predicted a group difference in theta-gamma PAC between groups.

461 Delta-theta PAC, delta-low gamma PAC and theta-low gamma PAC were computed over the  
462 entrainment period separately for each group by computing the respective modulation indices.

463 We then applied Wilcoxon rank sum tests to compare these modulation indices between the  
464 two groups. No significant differences were found for delta-theta PAC ( $z = -1.34$ ,  $p = 0.18$ ,

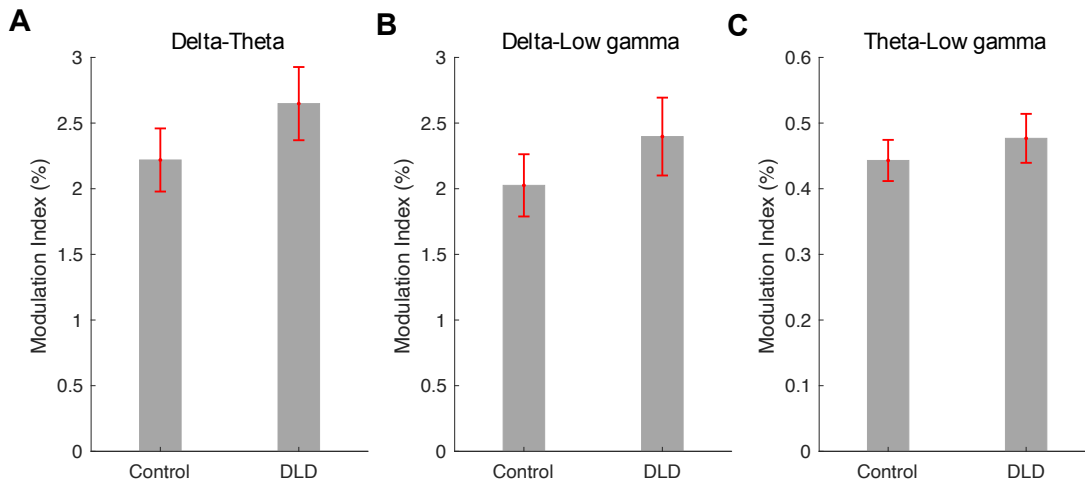
465 Figure 7A) or delta-low gamma PAC ( $z = -1.07$ ;  $p = 0.28$ , Figure 7B), nor for theta-low gamma

466 PAC (Wilcoxon rank sum test,  $z = -0.85$ ;  $p = 0.40$ , Figure 7C). Similar non-significant results

467 were found following outlier removal. Contrary to prediction, therefore, theta-gamma PAC was

468 not different in the children with DLD for the rhythmic syllable repetition task.

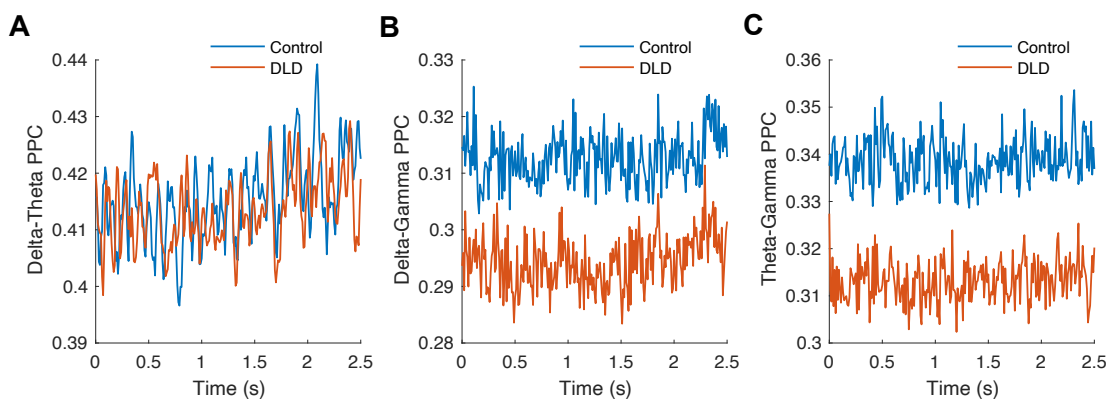
469



470  
471 **Figure 7. Modulation index was used as a measure for delta-theta (A), delta-low gamma**  
472 **(B), and theta-low gamma (C) phase-amplitude coupling.** The error bars denote the standard  
473 error of mean.  
474

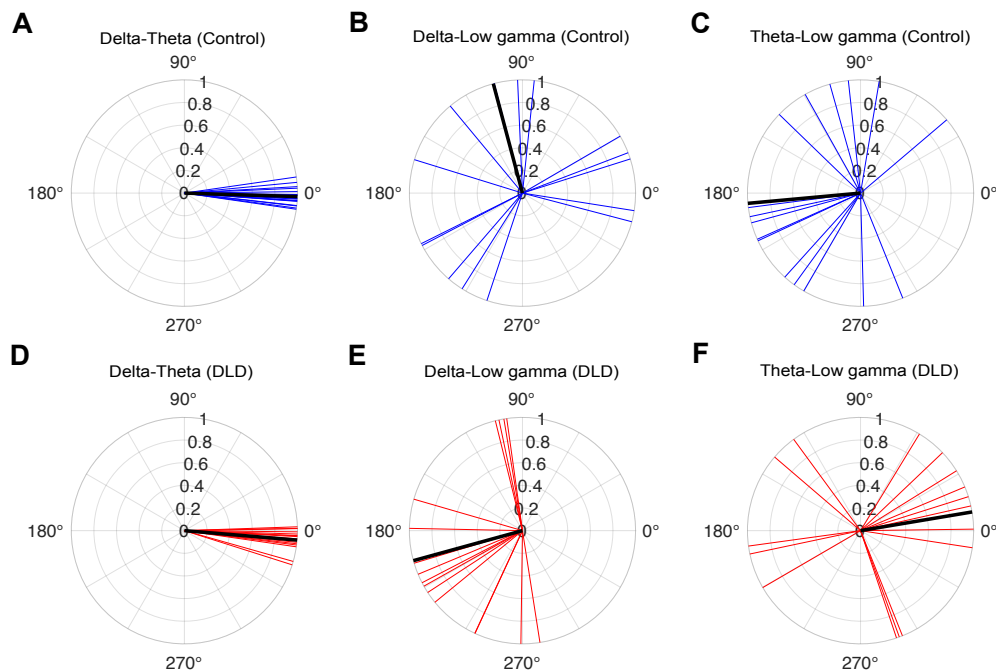
### 475 3.7. Comparing cross-frequency PPC between groups

476 Phase-phase coupling was also compared between groups. Delta-theta PPC, delta-low gamma  
477 PPC and theta-low gamma PPC were computed over the entrainment period separately for each  
478 group, as described in Section 2.9. We then applied two-sample t-tests to compare the two  
479 groups. As for PAC, no significant group differences were found, delta-theta PPC ( $p = 0.89$ ,  
480 Figure 8A), delta-low gamma PPC ( $p = 0.26$ , Figure 8B), theta-low gamma PPC ( $p = 0.11$ ,  
481 Figure 8C). Group PPC remained statistically equivalent after outlier removal.  
482



483  
484 **Figure 8. Delta-band (A), theta-band (B), and low gamma-band (C) phase-phase coupling.**  
485 The blue and red curves denote the PPCs for control and DLD groups, respectively.  
486

487 Finally, we calculated the phase difference (see Equation 8) for delta-theta, delta-low gamma,  
488 and theta-low gamma oscillations for each child at the onsets of stimuli (4th–8th) during the  
489 entrainment period. The resultant phase difference for each group was then computed by  
490 averaging across the phase differences obtained for children in that group, and separately for  
491 delta-theta, delta-low gamma, and theta-low gamma oscillations (see Figure 9). We applied  
492 Watson-Williams tests to compare the group resultant phases between the groups. All measures  
493 for both groups (TD and DLD) followed von Mises distributions (Watson’s U2 test,  $p > 0.05$ ).  
494 In this case, low-frequency resultant phase (delta and theta) did show significant differences  
495 between the two groups when coupling with the higher-frequency gamma band, delta-low  
496 gamma ( $p = 0.04$ ), theta-low gamma ( $p = 3.28 \times 10^{-4}$ ). Accordingly, the synchronisation of low-  
497 frequency phases (delta, theta) with high-frequency phase (low gamma) appears to operate  
498 differently for children with DLD. These differences are clearly visible in Figure 9. However,  
499 regarding delta-theta resultant phase differences, the two groups were not significantly different  
500 ( $p = 0.11$ ).



501  
502 **Figure 9. Delta-theta, delta-low gamma, and theta-low gamma resultant phase differences**  
503 **at the onsets of stimuli (4th–8th) during the entrainment period for control (A, B, C) and**  
504 **DLD (D, E, F) children.** The blue and red vectors denote the resultant phase difference for



505 individual children in control and DLD groups, respectively. The black vectors show the group  
506 resultant phase difference.

507

#### 508 **4. Discussion**

509 The current study investigated the ARR hypothesis of developmental disorders of language at  
510 the neural level, by examining different mechanistic aspects of the oscillatory encoding of a  
511 highly constrained rhythmic speech input, the repetition of the syllable “ba” at a 2 Hz rate.  
512 Despite the similarities in behavioural and sensory rhythm processing tasks that have been  
513 documented for children with DLD and children with dyslexia (Richardson et al., 2004;  
514 Corriveau et al., 2007; Thomson & Goswami, 2008; Corriveau & Goswami, 2009; Fraser et  
515 al., 2010; Goswami et al., 2011; Beattie & Manis, 2012; Goswami et al., 2013; Cumming et  
516 al., 2015a,b; Richards & Goswami, 2015, 2019), the neural mechanisms that were atypical for  
517 the children with DLD in this paradigm were quite different from those previously documented  
518 for children with dyslexia (Power et al., 2013; Keshavarzi et al., 2022). In particular, the  
519 expectation of impaired delta band responses for children with DLD was not supported. The  
520 children with DLD showed equivalent phase entrainment strength to TD children in the delta  
521 band, they showed equivalent preferred delta phase, and they showed equivalent delta band  
522 angular velocity. ERPs in the delta band did not differ by group, and nor did delta band power  
523 in the entrainment period. Similar results were found for the theta band regarding these  
524 parameters, with the exception that theta band power during the entrainment period was  
525 significantly elevated in DLD children (Figure 6). These data suggest that the delta and theta  
526 band mechanisms that are thought to underpin rhythmic speech encoding are operating in an  
527 essentially similar way in the DLD brain when compared to the brains of age-matched TD  
528 children, at least in the rhythmic syllable repetition task paradigm.

529 By contrast, low gamma band oscillatory responses in the rhythmic syllable repetition  
530 task showed some differences in the DLD brain. Low gamma band phase entrainment in the

531 children with DLD was absent in the current paradigm, suggesting that phase consistency in  
532 this band was not attained despite the highly predictable input. There was also a faster angular  
533 velocity in the gamma band for the DLD children, suggesting that gamma phase changed  
534 differently over time when compared to TD children. Furthermore, when low-frequency phases  
535 had to synchronise with high-frequency gamma responses in our task, there were group  
536 differences in resultant phase compared to the TD controls, for both delta-low gamma and  
537 theta-low gamma coupling (Figure 9). Although the strength of phase-amplitude and phase-  
538 phase coupling in the two groups of children was not significantly different (Figure 8), the  
539 resultant phase differences suggest that this similar synchronisation strength was generated by  
540 a different underlying relationship between low-frequency phase and high-frequency phase in  
541 the DLD brain. One way of interpreting the consequences for speech processing is that the  
542 interactions or connectivity between neural networks at these different rates is impaired,  
543 namely the theoretical notion of *communication through coherence* (Fries, 2015). Fries (2009,  
544 2015) proposed that neuronal inputs that arrive at random phases of the excitability cycle of  
545 related rhythmic neuronal responses will have lower effective connectivity, with consequently  
546 negative effects for cognition. Fries used examples from gamma band activity during visual  
547 cognition (primarily in animals) to illustrate communication through coherence, but the  
548 fundamental principle that he was proposing is relevant here, which is that the synchronization  
549 of brain oscillations is a key mechanism for information encoding and perceptual binding. In  
550 our data, the gamma rhythmic response to the highly predictable speech input does not attain  
551 phase consistency, making it more difficult for low-frequency responses (delta, theta) to  
552 synchronise their phases to gamma phase. This could suggest reduced coherence during speech  
553 processing, negatively affecting the precision of linguistic encoding. In communication  
554 through coherence theory, gamma-band coherence enables communication to be not only  
555 effective but also precise. Although some aspects of our data suggest that the low-frequency

556 responses (delta and theta) and their phase relations are operating in the same way as for TD  
557 children during the rhythmic speech task (with equivalent PAC and PPC strength), an optimal  
558 phase relation with gamma band responses in the temporal domain cannot be established,  
559 thereby impairing speech processing. This is mechanistically quite different from our previous  
560 findings with children with developmental dyslexia in this paradigm, where delta phase was  
561 atypical (Power et al., 2013; Keshavarzi et al., 2022). Nevertheless, for dyslexic children also,  
562 PAC mechanisms were explored and appear to be intact (delta-beta PAC, see Power et al., 2016;  
563 Keshavarzi et al., 2024).

564         A related view of the importance of gamma band processing for speech encoding  
565 concerns the parsing of phonemic information in the speech signal (Giraud & Poeppel, 2012;  
566 Poeppel, 2014). For example, it is known that speech contains crucial information required for  
567 successful linguistic decoding of the signal that is carried at multiple temporal scales, such as  
568 intonation-level or prosodic information at the scale of 500–2000 ms (argued to be encoded by  
569 delta band responses), syllabic information that is correlated to the acoustic envelope of speech  
570 at the scale of 150–300 ms (encoded by theta band responses), and rapidly-changing featural  
571 information at the scale of 20–80 ms (encoded by gamma band responses). One mechanism for  
572 encoding is suggested to be the sliding and resetting of neural temporal windows that match  
573 information in the signal via oscillatory responses, implemented as phase locking to key  
574 features of the input via phase-resetting of the intrinsic oscillations. While more recent work  
575 has shown that acoustic feature information is also encoded by the slower delta and theta band  
576 responses (for adults, children and infants, see Di Liberto et al., 2015, 2018, 2023), the idea  
577 that gamma band responses encode phoneme-relevant information has been supported by  
578 transcranial alternating current stimulation (tACS) studies using gamma band stimulation. For  
579 example, Marchesotti et al. (2020) reported that 20 minutes of tACS stimulation at ~30Hz  
580 significantly improved phonemic awareness in a behavioural task for French adults with

581 dyslexia. The data presented here may suggest that the ~30 Hz response to acoustic feature  
582 information in speech is atypical in the DLD brain, which could impair some aspects of  
583 phoneme awareness. However, given that most phonetic features are present in natural speech  
584 over much longer time windows (see Menn et al., 2023), and given that the cortex maintains  
585 representations of phonetic information even after it is lost from sensory input (Gwilliams et  
586 al., 2022), the idea that the gamma band differences reported here prevent children with DLD  
587 from representing phonemic information seems unlikely. Accordingly, we prefer to interpret  
588 the data using communication through coherence theory. Our findings appear to indicate  
589 reduced co-ordination of low-frequency oscillatory phase with gamma band responses in the  
590 DLD brain, reflecting altered neuronal network interactions during linguistic processing that  
591 may affect encoding precision and thereby impair speech perception at all phonological levels,  
592 not only the phoneme level. Converging studies with natural speech rather than the rhythmic  
593 speech paradigm utilised here are required to assess these different possibilities.

594         The gamma band differences reported here are also interesting with respect to an  
595 alternative auditory theory of DLD, the rapid auditory processing (RAP) theory (Tallal, 1980,  
596 2004). RAP theory proposed that basic auditory processing of brief, rapidly successive acoustic  
597 changes is impaired in children with DLD, drawing on data from a nonspeech task using brief  
598 (75 ms) pairs of tones that differed in pitch and succeeded each other rapidly in time (e.g., gaps  
599 of 8, 15, 30, 60 ms, see Tallal & Piercy, 1973). The children's task was to decide whether a  
600 high tone preceded a low tone in a pair or vice versa. Children with DLD were worse than TD  
601 controls in the tone task when the gap between stimuli was short, but were not different to TD  
602 controls when the gaps were longer (greater than 150 ms). Regarding speech processing, RAP  
603 difficulties were expected to affect phonetic discrimination (thought to require processing at  
604 rapid timescales around 40 ms, for example discriminating /b/ from /d/) via impaired  
605 discrimination of formant transitions (rapid acoustic changes in frequency and intensity).

606 Further, for children with DLD, intervention studies based on RAP can lead to improved  
607 language skills (e.g., Stevens et al., 2008, although see also Gillam et al., 2008).

608         Regarding neural data with DLD children, a nonspeech MEG study by Heim and  
609 colleagues indicated altered temporal organization of gamma-band oscillatory activity when  
610 children with DLD processed rapid tone sequences (Heim et al., 2011). Children listened to  
611 pairs of tones separated by 70 ms, and judged the pitch of the second tone. Heim et al. reported  
612 significantly reduced amplitude and phase-locking of early (45–75 ms) oscillations in the  
613 gamma-band range (29–52 Hz) for the second stimulus. ERP studies of infants at family risk  
614 for DLD using brief rapidly-presented tones have reported differences in auditory evoked  
615 potentials indexing change detection compared to TD infants, and in resting state gamma  
616 power, which in some studies predicted later language skills (English, language measured at 3,  
617 4 and 5 years, Benasich et al., 2008; Choudhury & Benasich, 2011; Gou et al., 2011; Italian,  
618 language measured at 20 months, Cantiani et al., 2016, 2019). Of particular interest regarding  
619 the current dataset, an investigation of the same English-exposed infants studied by Choudhury  
620 and Benasich (2011) at 6 and 12 months showed that the infant change detection response for  
621 rapidly-presented tone pairs was mainly determined by low frequency power and phase-locking  
622 responses (2-3 Hz, Hamalainen et al., 2019). Regarding the ARR hypothesis, it is logically  
623 possible that while children with both DLD and dyslexia share a difficulty in processing AE  
624 rise times and show difficulties in behavioural speech rhythm tasks, the rates of temporal  
625 integration that are impaired neurally may differ for each developmental disorder. These prior  
626 infant studies and the current gamma band data are consistent with Tallal's (2004) claim that  
627 auditory processing in temporal integration windows of around 40ms (25 Hz) is adversely  
628 affected in children with DLD. However, low frequency phase-phase mechanisms may  
629 contribute to this impaired processing. Further RAP studies based on processing natural speech

630 rather than pairs of tones are required to investigate this further, and to explore potential links  
631 to phoneme representation.

632         The current study has a number of limitations. Firstly, the rhythmic speech task is not  
633 a natural language task. Further investigation of the ARR hypothesis using natural speech  
634 listening tasks is required in order to establish whether the current gamma band and resultant  
635 phase differences are present during natural language processing. Second, the sample size is  
636 small, with 16 DLD children. However, it is representative of the existing neural DLD literature  
637 (e.g., Heim et al. 2011 studied 17 children with DLD, Choudhury & Benasich 2011 studied 17  
638 infants at risk for DLD). This reflects the difficulty of engaging families regarding  
639 neuroimaging.

640         In conclusion, here we find that the 9-year-old DLD brain does not show the delta-band  
641 deficits predicted by TS theory to underpin impaired rhythmic speech processing. Instead, the  
642 children with DLD exhibited an absence of phase consistency in the gamma band when  
643 processing highly predictable rhythmic speech, and showed different angular velocity in the  
644 gamma band compared to TD children. The children with DLD also showed significantly  
645 greater gamma and theta power during the task, and a difference in resultant phase when low-  
646 frequency phases (delta, theta) coupled with low gamma. These latter data are consistent with  
647 some prior neural nonspeech investigations of children with DLD. Overall, the data suggest  
648 reduced coherence between slower and faster networks during speech processing, which would  
649 negatively affect the precision of linguistic encoding. Further studies employing natural  
650 continuous speech are required to investigate this interpretation in more depth.

651

## 652 **Data and Code Availability**

653 Data and code will be made available on request.

654

## 655 **Author contributions**

656 M.K. conceptualisation, methodology, data collection, data analyses, visualisation, writing –  
657 original draft; S.R. data collection, writing – review & editing; G.F. data collection, writing –  
658 review & editing; L.P. data collection, writing – review & editing; U.G. funding acquisition,  
659 project administration, supervision, conceptualisation, methodology, writing – original draft.

660

## 661 **Conflict of interest**

662 The authors declare no conflicts of interest.

663

## 664 **Acknowledgements**

665 The authors would like to thank all the children, families and schools involved in the study.  
666 This research was funded by a donation to UG from the Yidan Prize Foundation. The sponsor  
667 played no role in the study design, data interpretation nor writing of the report.

668

## 669 **References**

670

671 Asaridou, S. S., & Watkins, K. E. (2022). Neural basis of speech and language impairments in  
672 development: the case of developmental language disorder. (In K. Cohen Kadosh, Ed.; *The*  
673 *Oxford Handbook of Developmental Cognitive Neuroscience*, pp. C19.S1–C19.S9). Oxford  
674 University Press.

675 Attaheri, A., Panayiotou, D., Phillips, A., Ní Choisdealbha, A., Di Liberto, G., Rocha, S.,  
676 Brusini, P., Mead, N., Flanagan, S., Olawole-Scott, H., & Goswami, U. (2022). Cortical  
677 tracking of sung speech in adults vs infants: a developmental analysis. *Frontiers in*  
678 *Neuroscience*, 16, 842447. <https://doi.org/10.3389/fnins.2022.842447>

679 Attaheri, A., Ní Choisdealbha, A., Di Liberto, G., Rocha, S., Brusini, P., Mead, N., Olawole-  
680 Scott, H., Boutris, P., Gibbon, S., Williams, I., Grey, C., Flanagan, S., M., & Goswami, U.  
681 (2022). Delta- and theta-band cortical tracking and phase-amplitude coupling to sung speech  
682 by infants. *Neuroimage*, 247, 118698. <https://doi.org/10.1016/j.neuroimage.2021.118698>

683 Attaheri, A., Ní Choisdealbha, A., Rocha, S., Brusini, P., Di Liberto, G., Mead, N., Olawole-  
684 Scott, H., Boutris, P., Gibbon, S., Williams, I., Grey, Alfaró e Oliveira, M., Brough, C.,  
685 Flanagan, S., M., & Goswami, U. (preprint). Infant low-frequency EEG cortical power, cortical  
686 tracking and phase-amplitude coupling predicts language a year later. bioRxiv  
687 2022.11.02.514963. <https://doi.org/10.1101/2022.11.02.514963>

- 688 Badcock, N. A., Bishop, D. V. M., Hardiman, M. J., Barry, J. G., & Watkins, K. E. (2012). Co-  
689 localisation of abnormal brain structure and function in specific language impairment. *Brain*  
690 *and Language*, 120, 3, 310-320. <https://doi.org/10.1016/j.bandl.2011.10.006>
- 691 Beattie, R., & Manis, F. (2012). Rise time perception in children with reading and combined  
692 reading and language difficulties. *Journal of Learning Disabilities*, 46(3), 200-209.  
693 <https://doi.org/10.1177/0022219412449421>
- 694 Bedoin, N., Brisseau, L., Molinier, P., Roch, D., & Tillmann, B. (2016). Temporally Regular  
695 Musical Primes Facilitate Subsequent Syntax Processing in Children with Specific Language  
696 Impairment. *Frontiers in Neuroscience*, 10, 245. <https://doi.org/10.3389/fnins.2016.00245>
- 697 Benasich, A.A., Gou, Z., Choudhury, N., & Harris, K.D. (2008). Early cognitive and language  
698 skills are linked to resting frontal gamma power across the first three years. *Behavioural Brain*  
699 *Research*, 195, 215-222. <https://doi.org/10.1016/j.bbr.2008.08.049>
- 700 Bishop, D. V. M. (2013). Uncommon Understanding: Development and Disorders of Language  
701 Comprehension in Children. Psychology Press, 288, eBook ISBN9781315804699.  
702 <https://doi.org/10.4324/9781315804699>
- 703 Bishop, D., Snowling, M., Thompson, P., & Greenhalgh, T. (2017). Phase 2 of CATALISE: a  
704 multinational and multidisciplinary Delphi consensus study of problems with language  
705 development: Terminology. *Journal of Child Psychology and Psychiatry*, 58(10), 1068-1080.  
706 <https://doi.org/10.1111/jcpp.12721>
- 707 Blomert, L., & Mitterer, H. (2004). The fragile nature of the speech-perception deficit in  
708 dyslexia: Natural vs. synthetic speech. *Brain and Language*, 89(1), 21-26.  
709 [https://doi.org/10.1016/S0093-934X\(03\)00305-5](https://doi.org/10.1016/S0093-934X(03)00305-5)
- 710 Boemio, A., Fromm, S., Braun, A., & Poeppel, D. (2005). Hierarchical and asymmetric  
711 temporal sensitivity in human auditory cortices. *Nature Neuroscience*, 8, 389-395.  
712 <https://doi.org/10.1038/nn1409>
- 713 Cantiani, C., Riva, V., Piazza, C., Bettoni, R., Molteni, M., Choudhury, N., Marino, C., &  
714 Benasich, A. A., (2016). Auditory discrimination predicts linguistic outcome in Italian infants  
715 with and without familial risk for language learning impairment. *Developmental Cognitive*  
716 *Neuroscience*, 20, 23-34. <https://doi.org/10.1016/j.dcn.2016.03.002>
- 717 Cantiani, C., Ortiz-Mantilla, S., Riva, V., Piazza, C., Bettoni, R., Musaccia, G., Molteni, M.,  
718 Marino, C., & Benasich, A. A., (2019). Reduced left-lateralized pattern of event-related EEG  
719 oscillations in infants at familial risk for language and learning impairment. *Neuroimage:*  
720 *Clinical*, 22, 101778. <https://doi.org/10.1016/j.nicl.2019.101778>
- 721 Choudhury, N. & Benasich, A. A. (2011). Maturation of auditory evoked potentials from 6 to  
722 48 months: Prediction to 3 – and 4 – year language and cognitive abilities. *Clinical*  
723 *Neurophysiology*, 122, 320-338. <https://doi.org/10.1016/j.clinph.2010.05.035>
- 724 Corriveau, K. H., & Goswami, U. (2009). Rhythmic motor entrainment in children with speech  
725 and language impairments: Tapping to the beat. *Cortex*, 45, 119-130.  
726 <https://doi.org/10.1016/j.cortex.2007.09.008>
- 727 Corriveau, K., Pasquini, E., & Goswami, U. (2007). Basic auditory processing skills and  
728 specific language impairment: A new look at an old hypothesis. *Journal of Speech, Language,*  
729 *and Hearing Research*, 50, 647-666. [https://doi.org/10.1044/1092-4388\(2007\)046](https://doi.org/10.1044/1092-4388(2007)046)



- 730 Cumming, R., Wilson, A., & Goswami, U. (2015). Basic auditory processing and sensitivity to  
731 prosodic structure in children with specific language impairments: A new look at a perceptual  
732 hypothesis. *Frontiers in Psychology*, 6, 972. <https://doi.org/10.3389/fpsyg.2015.00972>
- 733 Cumming, R., Wilson, A., Leong, V., Colling, L., & Goswami, U. (2015). Awareness of  
734 Rhythm Patterns in Speech and Music in Children with Specific Language Impairments.  
735 *Frontiers in Human Neuroscience*, 9. <https://doi.org/10.3389/fnhum.2015.00672>
- 736 Cutini, S., Szűcs, D., Mead, N., Huss, M., & Goswami, U. (2016). Atypical right hemisphere  
737 response to slow temporal modulations in children with developmental dyslexia. *NeuroImage*,  
738 143, 40-49. <https://doi.org/10.1016/j.neuroimage.2016.08.012>
- 739 Dauer, R. M. (1983). Stress-timing and syllable-timing reanalyzed. *Journal of Phonetics*, 11(1),  
740 51–62. [https://doi.org/10.1016/S0095-4470\(19\)30776-4](https://doi.org/10.1016/S0095-4470(19)30776-4)
- 741 Delorme, A., & Makeig, S. (2004). EEGLAB: an open-source toolbox for analysis of single-  
742 trial EEG dynamics including independent component analysis. *Journal of Neuroscience*  
743 *Methods*, 134(1), 9-21. <https://doi.org/10.1016/j.jneumeth.2003.10.009>
- 744 Di Liberto, G. M., Attaheri, A., Cantisani, G., Reilly, R. B., Ní Choisdealbha, A., Rocha, S.,  
745 Brusini, P., & Goswami, U. (2023). Emergence of the cortical encoding of phonetic features in  
746 the first year of life. *Nature Communications*, 14, 7789. [https://doi.org/10.1038/s41467-023-](https://doi.org/10.1038/s41467-023-43490-x)  
747 [43490-x](https://doi.org/10.1038/s41467-023-43490-x)
- 748 Di Liberto, G. M., Peter, V., Kalashnikova, M., Goswami, U., Burnham, D., & Lalor, E. C.,  
749 (2018). Atypical cortical entrainment to speech in the right hemisphere underpins phonemic  
750 deficits in dyslexia. *NeuroImage*, 175, 70-79.  
751 <https://doi.org/10.1016/j.neuroimage.2018.03.072>
- 752 Di Liberto, G.M., O'Sullivan, J.A., & Lalor, E.C. (2015). Low-frequency cortical entrainment  
753 to speech reflects phoneme-level processing. *Current Biology*, 25, 2457-2465.  
754 <https://doi.org/10.1016/j.cub.2015.08.030>
- 755 Flanagan, S., & Goswami, U. (2018). The role of phase synchronisation between low frequency  
756 amplitude modulations in child phonology and morphology speech tasks. *Journal of the*  
757 *Acoustical Society of America*, 143(3), 1366. <https://doi.org/10.1121/1.5026239>
- 758 Fraser, J., Goswami, U., & Conti-Ramsden, G. (2010). Dyslexia and specific language  
759 impairment: The role of phonology and auditory processing. *Scientific Studies of Reading*, 14,  
760 8-29. <https://doi.org/10.1080/10888430903242068>
- 761 Friedrich, M., & Friederici, D. (2005). Phonotactic Knowledge and Lexical-Semantic  
762 Processing in One-year-olds: Brain Responses to Words and Nonsense Words in Picture  
763 Contexts. *Journal of Cognitive Neuroscience*, 17(11), 1785-1802.  
764 <https://doi.org/10.1162/089892905774589172>
- 765 Friedrich, M., & Friederici, D. (2006). Early N400 development and later language acquisition.  
766 *Psychophysiology*, 43, 1, 1-12. <https://doi.org/10.1111/j.1469-8986.2006.00381.x>
- 767 Fries P. (2015). Rhythms for Cognition: Communication through Coherence. *Neuron*, 88(1),  
768 220-35. <https://doi.org/10.1016/j.neuron.2015.09.034>
- 769 Fries, P. (2009). The Model- and the Data-Gamma. *Neuron*, 64(5), 601-612.  
770 <https://doi.org/10.1016/j.neuron.2009.11.024>

- 771 Ghitza, O., & Greenberg, S. (2009). On the possible role of brain rhythms in speech perception:  
772 Intelligibility of time-compressed speech with periodic and aperiodic insertions of silence.  
773 *Phonetica*, 66, 113-126. <https://doi.org/10.1159/000208934>
- 774 Gillam, R.B., Loeb, D.F., Hoffman, L.M., Bohman, T., Champlin, C.A., Thibodeau, L., Widen,  
775 J., Brandel, J., & Friel-Patti, S. (2008). The efficacy of Fast ForWord language intervention in  
776 school-age children with language impairment: A randomized controlled trial. *Journal of*  
777 *Speech, Language, and Hearing Research*, 51(1), 97-119. [https://doi.org/10.1044/1092-4388\(2008/007\)](https://doi.org/10.1044/1092-4388(2008/007))
- 779 Giraud, A-L., & Poeppel, D. (2012). Cortical oscillations and speech processing: Emerging  
780 computational principles and operations. *Nature Neuroscience*, 15, 511-517.  
781 <http://dx.doi.org/10.1038/nn.3063>
- 782 Goswami, U. (2011). A temporal sampling framework for developmental dyslexia. *Trends in*  
783 *Cognitive Sciences*, 15(1), 3-10. <https://doi.org/10.1016/j.tics.2010.10.001>
- 784 Goswami, U. (2015). Sensory theories of developmental dyslexia: Three challenges for  
785 research. *Nature Reviews Neuroscience*, 16, 43-54. <http://dx.doi.org/10.1038/nrn3836>
- 786 Goswami, U. (2022). Language acquisition and speech rhythm patterns: an auditory  
787 neuroscience perspective. *Royal Society Open Science*, 9(7), 211855.  
788 <https://doi.org/10.1098/rsos.211855>
- 789 Goswami, U., & Leong, V. (2013). Speech rhythm and temporal structure: Converging  
790 perspectives?. *Laboratory Phonology*, 4(1), 67-92. <https://doi.org/10.1515/lp-2013-0004>
- 791 Goswami, U., Cumming, R., Chait, M., Huss, M., Mead, N., Wilson, A. M., Barnes, L., &  
792 Fosker, T. (2016). Perception of filtered speech by children with developmental dyslexia and  
793 children with specific language impairments. *Frontiers in Psychology*, 7, 791.  
794 <https://doi.org/10.3389/fpsyg.2016.00791>
- 795 Goswami, U., Mead, N., Fosker, T., Huss, M., Barnes, L., & Leong, V. (2013b). Impaired  
796 perception of syllable stress in children with dyslexia: A longitudinal study. *Journal of Memory*  
797 *and Language*, 69 (1), 1-17. <https://doi.org/10.1016/j.jml.2013.03.001>
- 798 Goswami, U., Wang, H-L. S., Cruz, A., Fosker, T., Mead, N., & Huss, M. (2011). Language-  
799 universal sensory deficits in developmental dyslexia: English, Spanish, and Chinese. *Journal*  
800 *of Cognitive Neuroscience*, 23, 325-337. <https://doi.org/10.1162/jocn.2010.21453>
- 801 Gou, Z., Choudhury, H., & Benasich, A.A. (2011). Resting frontal gamma power at 16, 24 and  
802 36 months predicts individual differences in language and cognition at 4 and 5 years.  
803 *Behavioural Brain Research*, 220, 263-270. <https://doi.org/j.bbr.2011.01.048>
- 804 Gramfort, A., Luessi, M., Larson, E., Engemann, D.A., Strohmeier, D., Brodbeck, C., Goj, R.,  
805 Jas, M., Brooks, T., Parkkonen, L., & Hämäläinen, M. (2013). MEG and EEG data analysis  
806 with MNE-Python. *Frontiers in neuroscience*, 267. <https://doi.org/10.3389/fnins.2013.00267>
- 807 Greenberg, S. (2006). A multi-tier framework for understanding spoken language. In S.  
808 Greenberg & W. Ainsworth (Eds.), *Listening to speech: An auditory perspective*. Lawrence  
809 Erlbaum Associates.
- 810 Gross, J., Hoogenboom, N., Thut, G., Schyns, P., Panzeri, S., Belin, P., & Garrod, S. (2013).  
811 Speech rhythms and multiplexed oscillatory sensory coding in the human brain. *PLOS Biology*,  
812 11(12), e1001752. <https://doi.org/10.1371/journal.pbio.1001752>

- 813 Gwilliams, L., King, J. R., Marantz, A., & Poeppel, D. (2022). Neural dynamics of phoneme  
814 sequences reveal position-invariant code for content and order. *Nature Communications*, 13,  
815 6606. <https://doi.org/10.1038/s41467-022-34326-1>
- 816 Hämäläinen, J. A., Ortiz-Mantilla, S. and Benasich, A., 2019. Change detection to tone pairs  
817 during the first year of life—Predictive longitudinal relationships for EEG-based source and  
818 time-frequency measures. *NeuroImage*, 198, 83-92.  
819 <https://doi.org/10.1016/j.neuroimage.2019.05.034>
- 820 Heim, S., Friedman, J.T., Keil, A., Benasich, A.A. (2011). Reduced Sensory Oscillatory  
821 Activity during Rapid Auditory Processing as a Correlate of Language-Learning Impairment.  
822 *Journal of Neurolinguistics*, 24(5), 539-555. <https://doi.org/10.1016/j.jneuroling.2010.09.006>
- 823 Helenius, P., Parviainen, T., Paetau, R., & Salmelin, R. (2009). Neural processing of spoken  
824 words in specific language impairment and dyslexia. *Brain*, 132, 7, 1918-1927.  
825 <https://doi.org/10.1093/brain/awp134>
- 826 Helenius, P., Sivonen, P., Parviainen, T., Isoaho, P., Hannus, S., Kauppila, T., Salmelin, R., &  
827 Isotalo, L. (2014). Abnormal functioning of the left temporal lobe in language-impaired  
828 children. *Brain and Language*, 130, 11-18. <https://doi.org/10.1016/j.bandl.2014.01.005>
- 829 Hülsemann, M., Naumann, E., & Rasch, B. (2019). Quantification of Phase-Amplitude  
830 Coupling in Neuronal Oscillations: Comparison of Phase-Locking Value, Mean Vector Length,  
831 Modulation Index, and Generalized-Linear-Modeling-Cross-Frequency-Coupling. *Frontiers in*  
832 *Neuroscience*, 13, 573. <https://doi.org/10.3389/fnins.2019.00573>
- 833 Keshavarzi, M., Mandke, K., Macfarlane, A., Parvez, L., Gabrielczyk F., Wilson, A., &  
834 Goswami, U. (2022). Atypical Delta-band Phase Consistency and Atypical Preferred Phase in  
835 Children with Dyslexia during Neural Entrainment to Rhythmic Audio-Visual Speech.  
836 *NeuroImage: Clinical*, 35, 103054. <https://doi.org/10.1016/j.nicl.2022.103054>
- 837 Keshavarzi, M., Mandke, K., Macfarlane, A., Parvez, L., Gabrielczyk F., Wilson, A., &  
838 Goswami, U. (2024). Atypical beta-band effects in children with dyslexia in response to  
839 rhythmic audio-visual speech. *Clinical Neurophysiology*, 1388-2457,  
840 <https://doi.org/10.1016/j.clinph.2024.02.008>
- 841 Keshavarzi, M., Ní Choisdealbha, A., Attaheri, A., Rocha, S., Brusini, P., Gibbon, S., Boutris,  
842 P., Mead, N., Olawole-Scott, H., Ahmed, H., Flanagan, S., Mandke, K., & Goswami, U. (2024).  
843 Decoding speech information from EEG data with 4-, 7- and 11-month-old infants: Using  
844 convolutional neural network, mutual information-based and backward linear models. *Journal*  
845 *of Neuroscience Methods*, 403, 110036. <https://doi.org/10.1016/j.jneumeth.2023.110036>
- 846 Kotz, S., & Schmidt-Kassow, M. (2015). Basal ganglia contribution to rule expectancy and  
847 temporal predictability in speech. *Cortex*, 68, 48-60.  
848 <https://doi.org/10.1016/j.cortex.2015.02.021>
- 849 Ladányi, E., Persici, V., Fiveash, A., Tillmann, B., & Gordon, R. L. (2020). Is atypical rhythm  
850 a risk factor for developmental speech and language disorders?. *Wiley Interdisciplinary*  
851 *Reviews: Cognitive Science*, 11(5), e1528. <https://doi.org/10.1002/wcs.1528>
- 852 Lallier, M., Molinaro, N., Lizarazu, M., Bourguignon, M., & Carreiras, M. (2017). Amodal  
853 Atypical Neural Oscillatory Activity in Dyslexia: A Cross-Linguistic Perspective. *Clinical*  
854 *Psychological Science*, 5(2), 379-401. <https://doi.org/10.1177/2167702616670119>

- 855 Lee, J. C., Nopoulos, P. C., & Tomblin, J. B. (2013). Abnormal subcortical components of the  
856 corticostriatal system in young adults with DLI: a combined structural MRI and DTI study.  
857 *Neuropsychologia*, 51(11), 2154-2161.  
858 <https://doi.org/10.1016/j.neuropsychologia.2013.07.011>
- 859 Leonard, L.B. (2014). Children with specific language impairment. *Cambridge, MA: MIT*  
860 *Press*. <https://doi.org/10.7551/mitpress/9152.001.0001>.
- 861 Leong, V., & Goswami, U. (2015). Acoustic-emergent phonology in the amplitude envelope of  
862 child-directed speech. *PLOS ONE*, 10(12), e0144411. [https://doi.org/10.1371/journal](https://doi.org/10.1371/journal.pone.0144411)  
863 [.pone.0144411](https://doi.org/10.1371/journal.pone.0144411)
- 864 Manis, F. R., McBride-Chang, C., Seidenberg, M. S., Keating, P., Doi, L. M., Munson, B., &  
865 Petersen, A. (1997). Are speech perception deficits associated with developmental dyslexia?.  
866 *Journal of experimental child psychology*, 66(2), 211-235. [https://doi.org/](https://doi.org/10.1006/jecp.1997.2383)  
867 [10.1006/jecp.1997.2383](https://doi.org/10.1006/jecp.1997.2383)
- 868 Marchesotti, S., Nicolle, J., Merlet, I., Arnal, L. H., Donoghue, J. P., & Giraud, A-L. (2020).  
869 Selective enhancement of low gamma activity by tACS improves phonemic processing and  
870 reading accuracy in dyslexia. *PLoS Biology*, 18(9), e3000833.  
871 <https://doi.org/10.1371/journal.pbio.3000833>
- 872 Mehta, B., Chawla, V. K., Parakh, M., Parakh, P., Bhandari, B., & Gurjar, A. S. (2015). EEG  
873 Abnormalities in Children with Speech and Language Impairment. *Journal of Clinical and*  
874 *Diagnostic Research*, 9(7), CC04. <https://doi.org/10.7860/JCDR/2015/13920.6168>
- 875 Menn, K. H., Männel, C., & Meyer, L. (2023). Phonological acquisition depends on the timing  
876 of speech sounds: Deconvolution EEG modeling across the first five years. *Science Advances*,  
877 9(44), eadh2560. <https://doi.org/10.1126/sciadv.adh2560>
- 878 Ní Choisdealbha, A., Attaheri, A., Rocha, S., Brusini, P., Flanagan, S., M., Mead, N., Gibbon,  
879 S., Olawole-Scott, H., Williams, I., Grey, C., Boutris, P., Ahmed, H., & Goswami, U. (2022).  
880 Neural detection of changes in amplitude rise time in infancy. *Developmental Cognitive*  
881 *Neuroscience*, 54, 101075. <https://doi.org/10.1016/j.dcn.2022.101075>
- 882 Ní Choisdealbha, A., Attaheri, A., Rocha, S., Mead, N., Olawole-Scott, H., Brusini, P., Gibbon,  
883 S., Boutris, P., Grey, C., Hines, D., Williams, I., Flanagan, S., & Goswami, U. (2023). Neural  
884 phase angle from two months when tracking speech and non-speech rhythm linked to language  
885 performance from 12 to 24 months. *Brain and Language*, 243, 105301.  
886 <https://doi.org/10.1016/j.bandl.2023.105301>
- 887 Ortiz-Mantilla, S., & Benasich, A. (2013). Neonatal electrophysiological predictors of  
888 cognitive and language development. *Developmental Medicine & Child Neurology*, 55(9), 781-  
889 782. <https://doi.org/10.1111/dmcn.12207>
- 890 Parker, A. J., Woodhead, Z. V. J., Carey, D. P., Groen, M. A., Gutierrez-Sigut, E., Hodgson,  
891 Hudson, J., Karlsson, E. M., MacSweeney, M., Payne, H., Simpson, N., Thompson, P. A.,  
892 Watkins, K. E., Egan, C., Grant, J. H., Harte, S., Hudson, B. T., Sablik, M., Badcock, N. A., &  
893 Bishop, D. V. M. (2022). Inconsistent language lateralisation Testing the dissociable language  
894 laterality hypothesis using behaviour and lateralised cerebral blood flow. *Cortex*, 154, 105-134.  
895 <https://doi.org/10.1016/j.cortex.2022.05.013>
- 896 Parvez, L., Keshavarzi, M., Richards, S., Di Liberto, G. M., & Goswami, U. (2024). Atypical  
897 speech production of multisyllabic items by children with developmental language disorder  
898 (DLD) indicate prosodic difficulties. *PsyArXiv*. <https://doi.org/10.31234/osf.io/52r6h>

- 899 Peter, V., van Ommen, S., Kalashnikova, M., Mazuka, R., Nazzi, T., & Burnham, D. (2022).  
900 Language specificity in cortical tracking of speech rhythm at the mora, syllable, and foot levels.  
901 *Scientific Reports*, 12, 13477. <https://doi.org/10.1038/s41598-022-17401-x>
- 902 Poeppel, D. (2014). The neuroanatomic and neurophysiological infrastructure for speech and  
903 language. *Current Opinion in Neurobiology*, 28, 142-149.  
904 <https://doi.org/10.1016/j.conb.2014.07.005>
- 905 Power, A. J., Colling, L. C., Mead, N., Barnes, L., & Goswami, U. (2016). Neural encoding of  
906 the speech envelope by children with developmental dyslexia. *Brain & Language*, 160, 1-10.  
907 <https://doi.org/10.1016/j.bandl.2016.06.006>
- 908 Power, A. J., Mead, N., Barnes, L., & Goswami, U. (2012). Neural entrainment to rhythmically  
909 presented auditory, visual, and audio-visual speech in children. *Frontiers in Psychology*, 3, 216.  
910 <https://doi.org/10.3389/fpsyg.2012.00216>
- 911 Power, A. J., Mead, N., Barnes, L., & Goswami, U. (2013). Neural entrainment to rhythmic  
912 speech in children with developmental dyslexia. *Frontiers in Human Neuroscience*, 7(777), 1-  
913 19. <https://doi.org/10.3389/fnhum.2013.00777>
- 914 Przybylski, L., Bedoin, N., Krifi-Papoz, S., Herbillon, V., Roch, D., & Léculier, L., Kotz, S. A.,  
915 & Tillmann, B. (2013). Rhythmic auditory stimulation influences syntactic processing in  
916 children with developmental language disorders. *Neuropsychology*, 27(1), 121-131.  
917 <https://doi.org/10.1037/a0031277>
- 918 Richards, S., & Goswami, U. (2015). Auditory processing in specific language impairment  
919 (SLI): Relations with the perception of lexical and phrasal stress. *Journal of Speech, Language,  
920 and Hearing Research*, 58(4), 1292-1305. [https://doi.org/10.1044/2015\\_jslhr-1-13-0306](https://doi.org/10.1044/2015_jslhr-1-13-0306)
- 921 Richards, S., & Goswami, U. (2019). Impaired recognition of metrical and syntactic boundaries  
922 in children with developmental language disorders. *Brain Sciences*, 9(2), 33.  
923 <https://doi.org/10.3390/brainsci9020033>
- 924 Richardson, U., Thomson, J. M., Scott, S. K., & Goswami, U. (2004). Auditory processing  
925 skills and phonological representation in dyslexic children. *Dyslexia*, 10, 215-233.  
926 <https://doi.org/10.1002/dys.276>
- 927 Ríos-López, P., Molinaro, N., Bourguignon, M., & Lallier, M. (2020). Development of neural  
928 oscillatory activity in response to speech in children from 4 to 6 years old. *Developmental  
929 Science*, 23(6), e12947. <https://doi.org/10.1111/desc.12947>
- 930 Rios-Lopez, P., Molinaro, N., Bourguignon, M., & Lallier, M. (2022). Right-hemisphere  
931 coherence to speech at pre-reading stages predicts reading performance one year later. *Journal  
932 of Cognitive Psychology*, 34, 2, 179-193. <https://doi.org/10.1080/20445911.2021.1986514>
- 933 Rocha, S., Ní Choisdealbha, A., Attaheri, A., Mead, N., Olawole-Scott, H., Grey, C., Williams,  
934 I., Gibbon, S., Boutris, P., Brusini, P., & Goswami, U. (in press). Language Acquisition in the  
935 Longitudinal Cambridge UK BabyRhythm Cohort. *Collabra: Psychology*, 10(1).  
936 <https://doi.org/10.1525/collabra.92998>
- 937 Sallat, S., & Jentschke, S. (2015). Music perception influences language acquisition: Melodic  
938 and rhythmic-melodic perception in children with specific language impairment. *Behavioural  
939 Neurology*, 2015, 606470. <https://doi.org/10.1155/2015/606470>

- 940 Serniclaes, W., van Heghe, S., Mousty, P., Carré, R., & Sprenger-Charolles, L. (2004).  
941 Allophonic mode of speech perception in dyslexia. *Journal of Experimental Child Psychology*,  
942 87, 336-361. <https://doi.org/10.1016/j.jecp.2004.02.001>
- 943 Shafer, V. L., Schwartz, R. G., Morr, M. L., Kessler, K. L., Kurtzberg, D., & Ruben, R. J. (2001)  
944 Neurophysiological Indices of Language Impairment in Children. *Acta Oto-Laryngologica*,  
945 121(2), 297-300. <https://doi.org/10.1080/000164801300043929>
- 946 Snowling, M. J. (2000). *Dyslexia* (2nd ed.). Oxford: Blackwell Publishers.
- 947 Stanovich, K. (1988). Explaining the differences between the dyslexic and the garden-variety  
948 poor reader: The Phonological-Core Variable-Difference Model. *Journal of Learning*  
949 *Disabilities*, 21, 590-604. <https://doi.org/10.1177/002221948802101003>
- 950 Stevens, C., Fanning, J., Coch, D., Sanders, L., & Neville, H. (2008). Neural mechanisms of  
951 selective auditory attention are enhanced by computerized training: electrophysiological  
952 evidence from language-impaired and typically developing children. *Brain research*, 1205, 55-  
953 69. <https://doi.org/10.1016/j.brainres.2007.10.108>
- 954 Swan, D., & Goswami, U. (1997). Phonological awareness deficits in developmental dyslexia  
955 and the phonological representations hypothesis. *Journal of Experimental Child Psychology*,  
956 66(1), 18-41. <https://doi.org/10.1006/jecp.1997.2375>
- 957 Systad, S., Bjørnvold, M., Sørensen, C., & Halaas Lyster, S. S. (2019). The value of  
958 electroencephalogram in assessing children with speech and language impairments. *Journal of*  
959 *Speech, Language, and Hearing Research*, 62(1), 153-168.  
960 [https://doi.org/10.1044/2018\\_JSLHR-L-17-0087](https://doi.org/10.1044/2018_JSLHR-L-17-0087)
- 961 Tallal, P. (1980). Auditory temporal perception, phonics, and reading disabilities in children.  
962 *Brain and Language*, 9, 182-198. [https://doi.org/10.1016/0093-934X\(80\)90139-X](https://doi.org/10.1016/0093-934X(80)90139-X)
- 963 Tallal, P. (2004). Improving language and literacy is a matter of time. *Nature Reviews*  
964 *Neuroscience*, 5, 721-728. <https://doi.org/10.1038/nrn1499>
- 965 Tallal, P. (2004). Improving language and literacy is a matter of time. *Nature Reviews*  
966 *Neuroscience*, 5, 721-728. <https://doi.org/10.1038/nrn1499>
- 967 Tallal, P., & Piercy, M. (1973). Defects of non-verbal auditory perception in children with  
968 developmental aphasia. *Nature*, 241, 468-469. <https://doi.org/10.1038/241468a0>
- 969 Thomson, J. M., & Goswami, U. (2008). Rhythmic processing in children with developmental  
970 dyslexia: Auditory and motor rhythms link to reading and spelling. *Journal of Physiology-*  
971 *Paris*, 102, 120-129. <https://doi.org/10.1016/j.jphysparis.2008.03.007>
- 972 Tort, A. B. L., Kramer, M. A., Thorn, C., & Kopell, N. J. (2008). Dynamic cross-frequency  
973 couplings of local field potential oscillations in rat striatum and hippocampus during  
974 performance of a T-maze task. *Proceedings of the National Academy of Sciences*, 105(51)  
975 20517-20522. <https://doi.org/10.1073/pnas.081052410>
- 976 Watkins, K. E., Vargha-Khadem, F., Ashburner, J., Passingham, R. E., Connelly, A., Friston, K.  
977 J., Frackowiak, R. S. J., Mishkin, M., & Gadian, D. G. (2002). MRI analysis of an inherited  
978 speech and language disorder: structural brain abnormalities. *Brain*, 125(3), 465-478.  
979 <https://doi.org/10.1093/brain/awf057>
- 980 Wechsler, D. (2016). Wechsler Intelligence Scale for Children, 4th Edn. London, UK: Pearson  
981 Assessment.

982 Wiig, E. H., Semel, E., Secord, W. A. (2017). Clinical Evaluation of Language Fundamentals  
983 - Fifth Edition. Pearson.